

Compaction Localization, Elastic-Plastic Coupling, and Constitutive Modeling of Castlegate Sandstone Deformation

DOE Basic Research Relevant to Geological CO₂ Sequestration

March 12, 2008

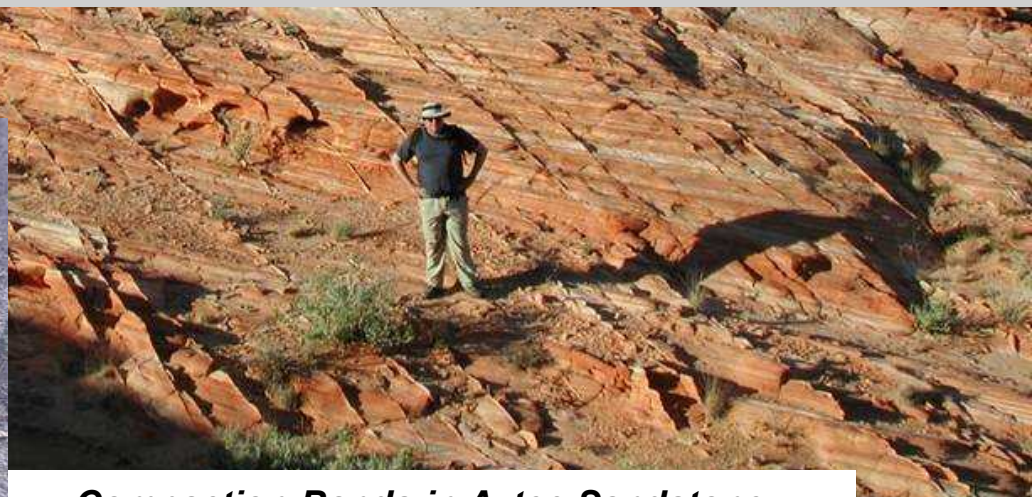
**Thomas Dewers¹, Kathleen Issen², David Holcomb¹ and William
Olsson¹**

¹**Sandia National Laboratories, Geomechanics, Albuquerque, NM**

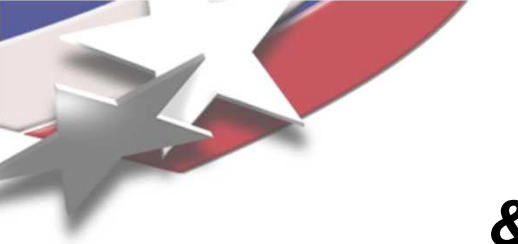
²**Clarkson University, Wallace H. Coulter School of Engineering, Potsdam, NY**



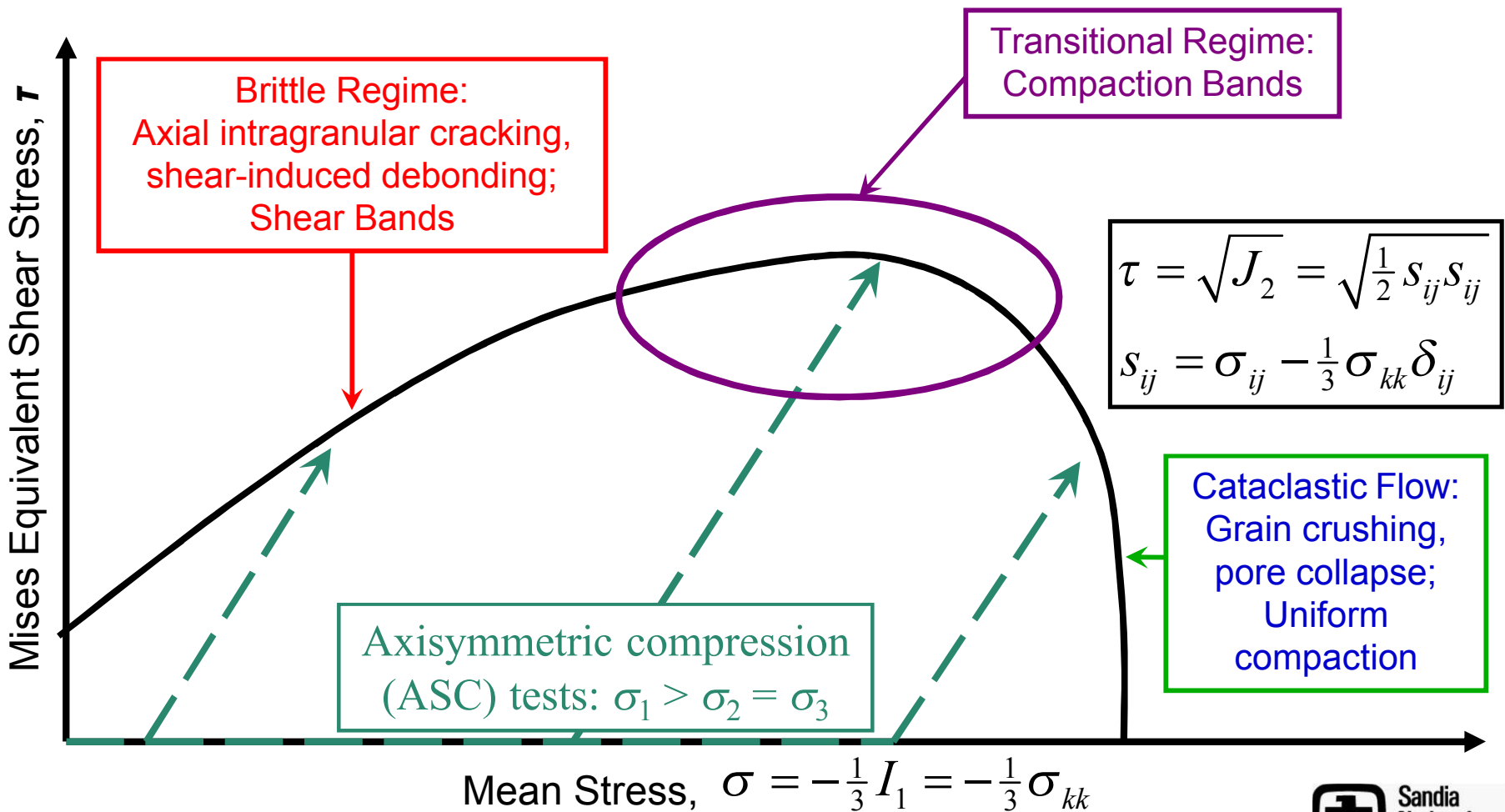
- **Overview**
- **Localization Theory**
- **Castlegate Ss Experimental Summary**
- **Determining Elastic and Plastic Strains**
- **Localization Predictions vs. Observations**
- **Modeling Castlegate Elasto-Plasticity**



**Compaction Bands in Aztec Sandstone,
from Sternlof et al., 2004**



Microstructural Deformation & Failure Modes In Sandstones

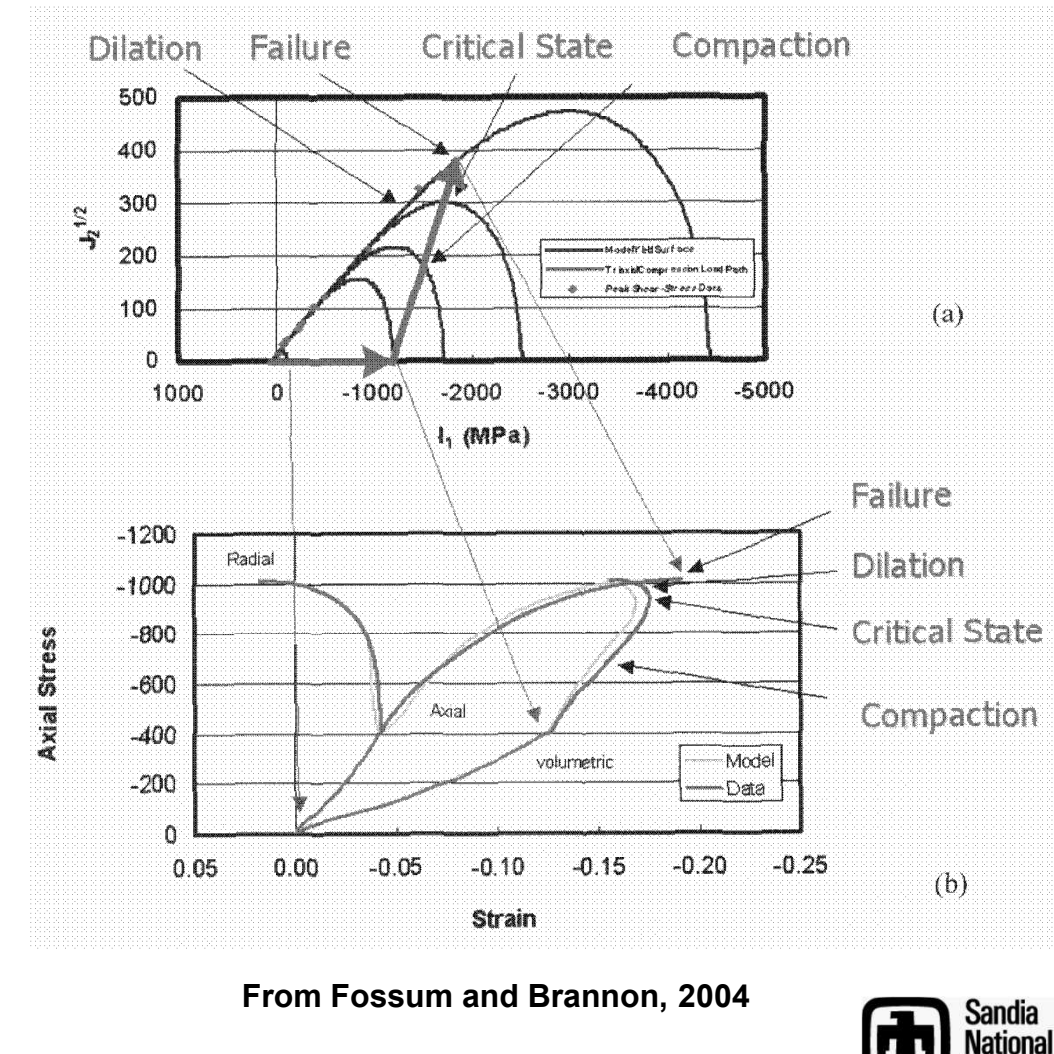
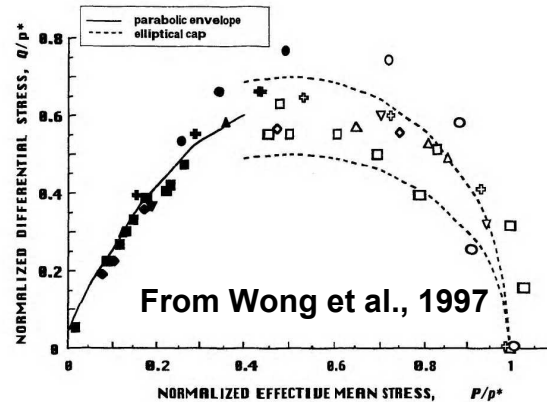
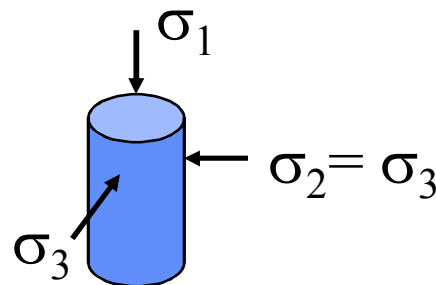


Overview of “Cap” Plasticity

Axisymmetric Compression Tests

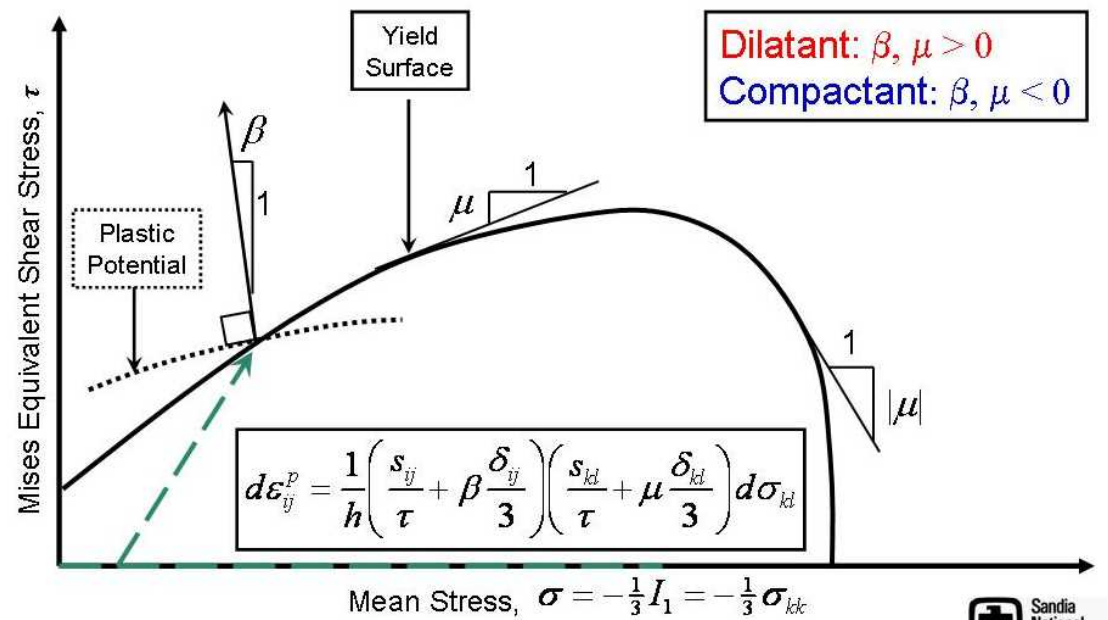
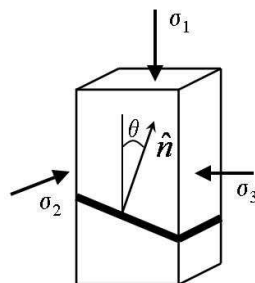
$$\sigma = I_1/3 = (\sigma_1 + 2 \sigma_3)/3$$

$$\tau = J_2^{1/2} = (\sigma_1 - \sigma_3)/(3^{1/2})$$



Localization Theory

- Derives from Rudnicki and Rice (1975) formulation
- Models formation of a planar band of localized strain
- Inception of band is bifurcation from homogeneous deform.
- Attributable to a constitutive instability
 - Single yield surface (depends on I_1 and J_2)
 - Non-associated flow



Predicts mode of occurrence and band angle, θ

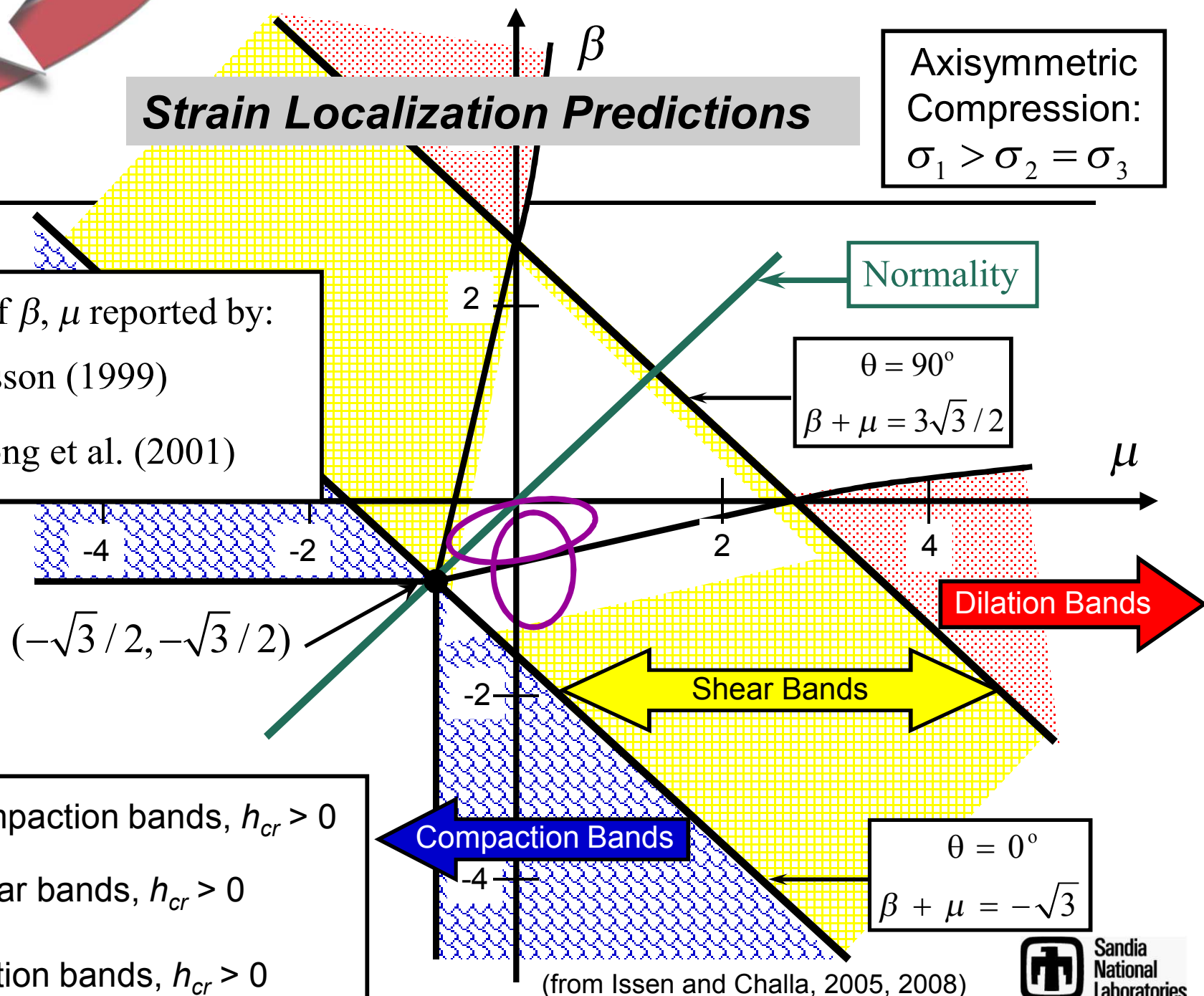
Strain Localization Predictions

Axisymmetric Compression:
 $\sigma_1 > \sigma_2 = \sigma_3$

Values of β, μ reported by:

○ Olsson (1999)

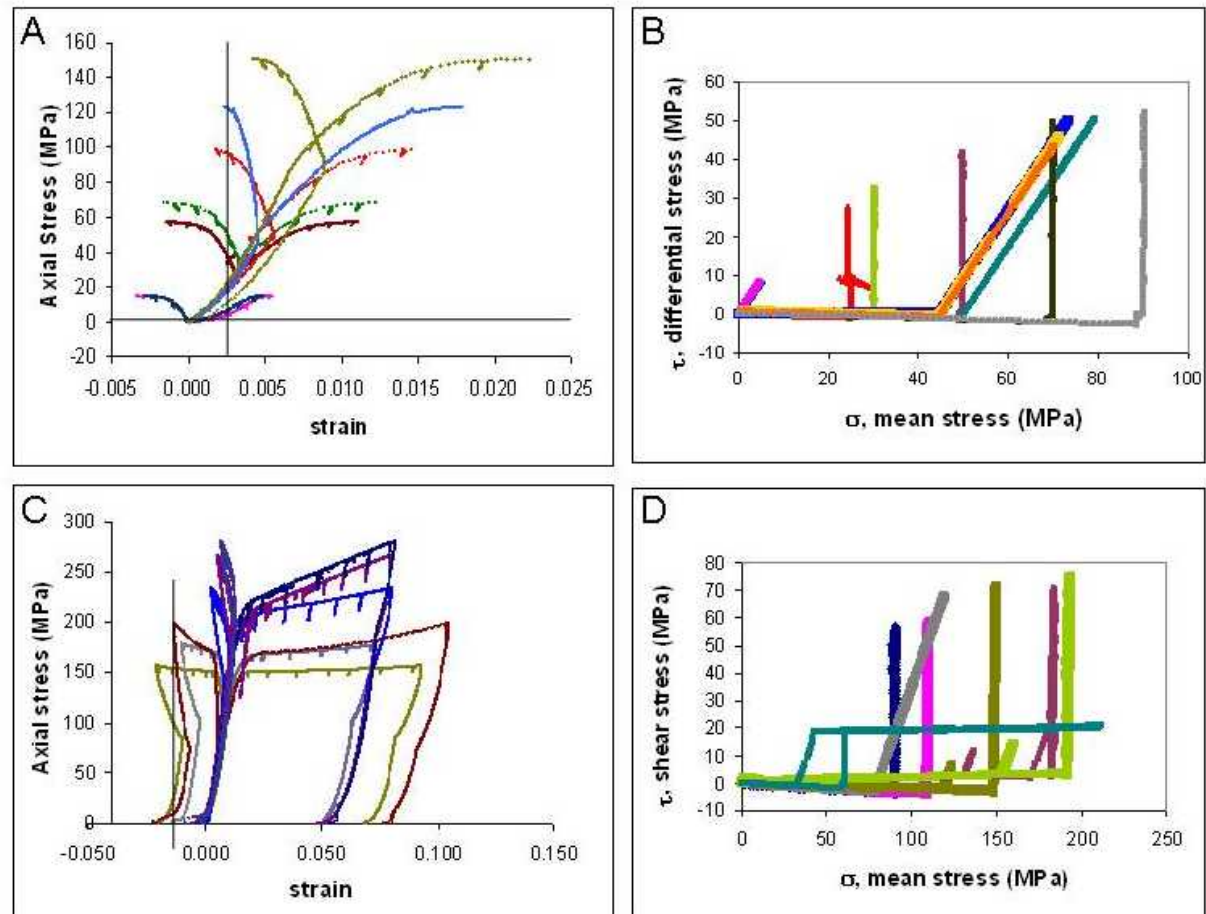
○ Wong et al. (2001)



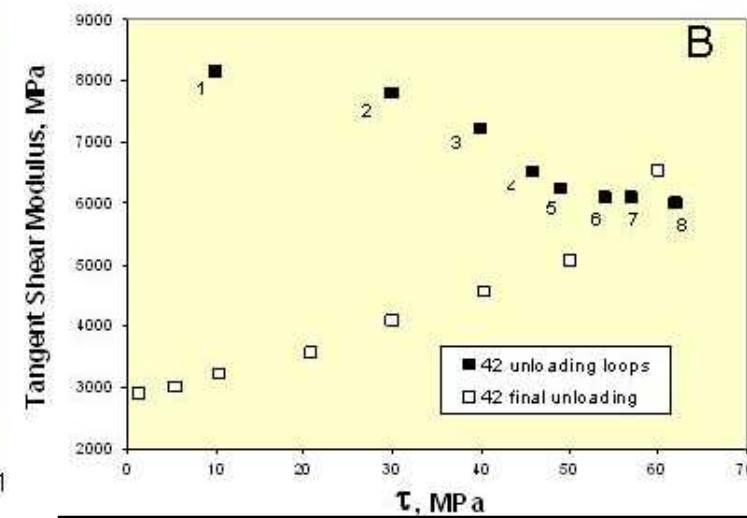
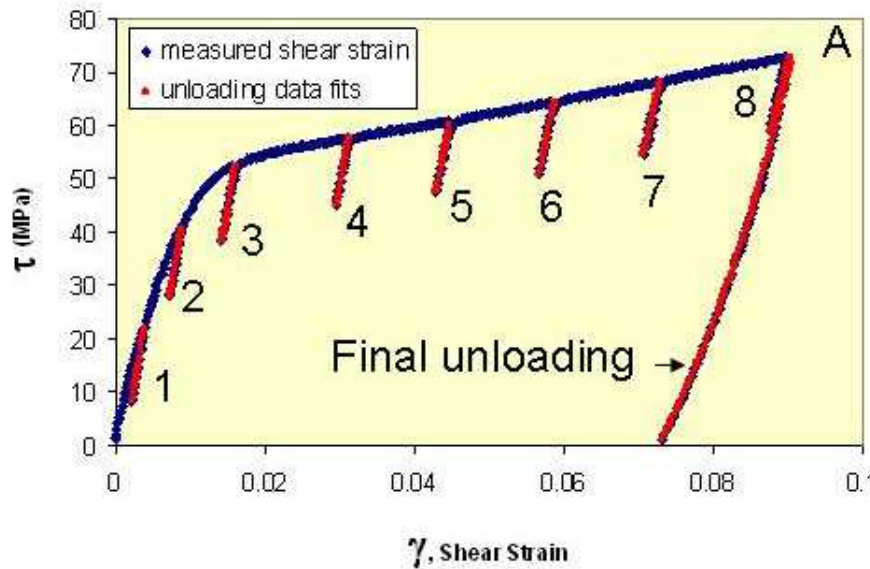
Castlegate Ss Experimental Summary

- Porosity ~ 28%
- Fine to medium grained (~0.2mm)
- 70-80% quartz
- Weakly lithified
- Studied previously

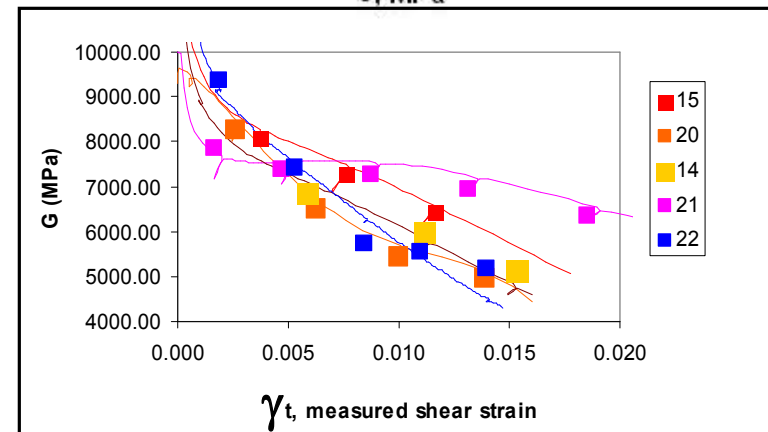
(Vinegar et al., 1991; Olsson and Holcomb, 2000; DiGiovanni et al., 2001; Holcomb and Olsson, 2003)



Elastic Moduli: Stress and Strain Dependence

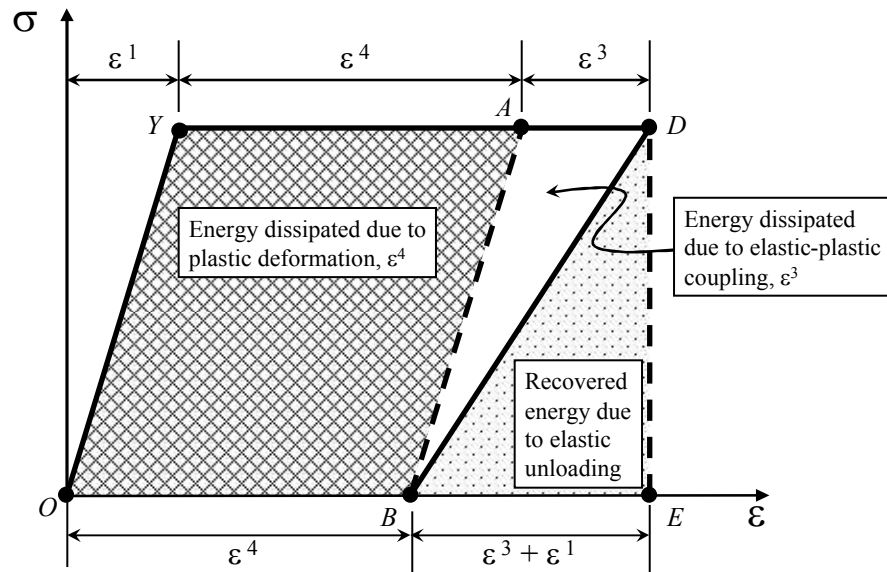


- Shear modulus G is local slope of τ - γ curves for unloading loops and final unloading, at constant mean stress.
- G decreases with γ_p at constant τ , and increases with τ at constant γ_p .



Observed and modeled G degradation with total shear strain

Incremental Strains and Elastic-Plastic Coupling



Schematic of uniaxial loading of an elastic-perfectly plastic material with elastic-plastic coupling (modulus decreases due to plastic strain). Elastic strain for the original modulus is ε^1 , plastic strain is ε^4 , and coupled strain is ε^3 (ε^2 is ignored here for simplicity).

$$\dot{\varepsilon}_{ij} = \dot{\varepsilon}_{ij}^1 + \dot{\varepsilon}_{ij}^2 + \dot{\varepsilon}_{ij}^3 + \dot{\varepsilon}_{ij}^4$$

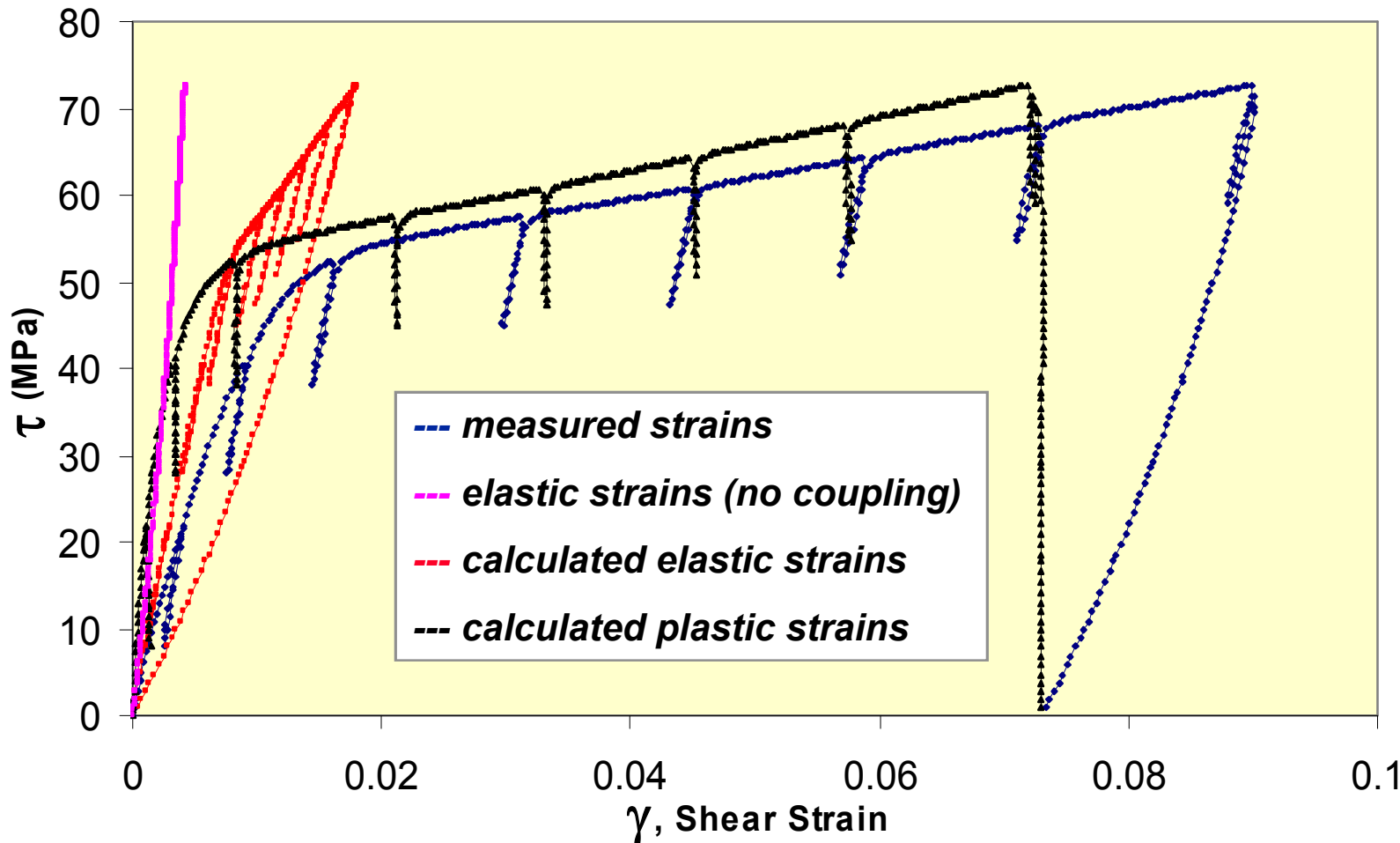
$$\dot{\varepsilon}_{ij}^1 = C_{ijkl} \dot{\sigma}_{kl}$$

$$\dot{\varepsilon}_{ij}^2 = \frac{\partial C_{ijkl}}{\partial \sigma_{mn}} \sigma_{kl} \dot{\sigma}_{mn}$$

$$\dot{\varepsilon}_{ij}^3 = \frac{\partial C_{ijkl}}{\partial \varepsilon_{mn}^p} \sigma_{kl} \dot{\varepsilon}_{mn}^p$$

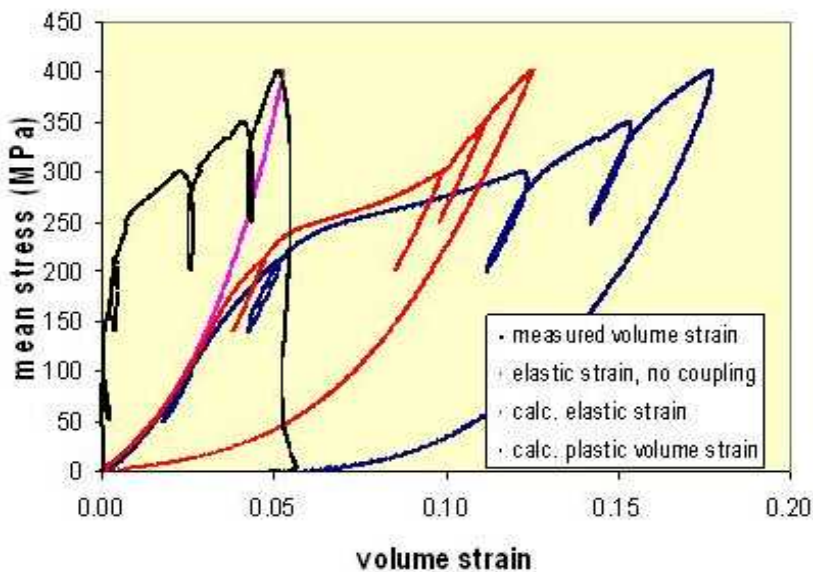
$$\dot{\varepsilon}_{ij}^4 = \dot{\varepsilon}_{ij}^p \text{ (plastic strain)}$$

Partitioning Strain into Elastic and Plastic Portions



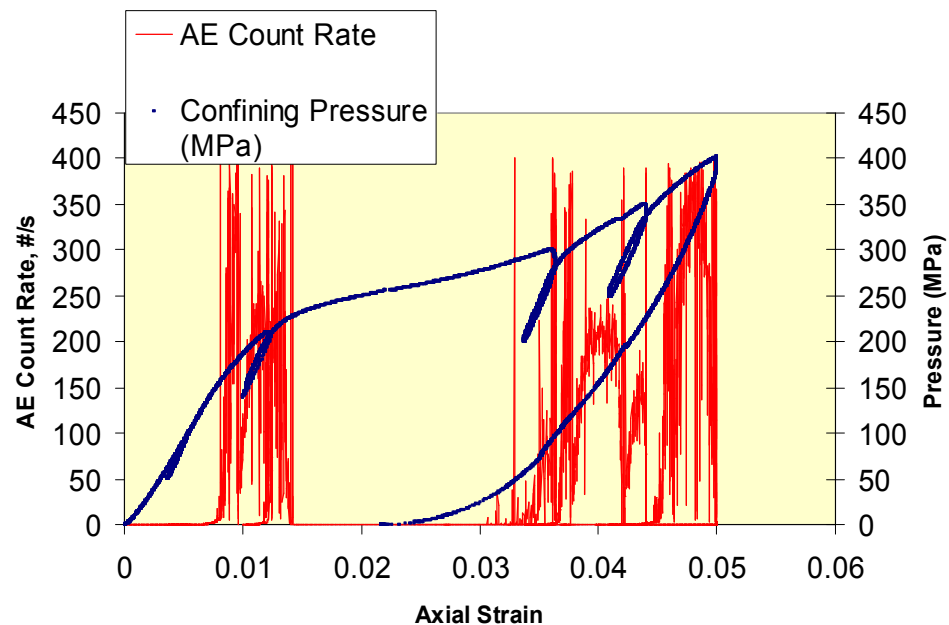


Strain Partitioning During Hydrostatic Compression

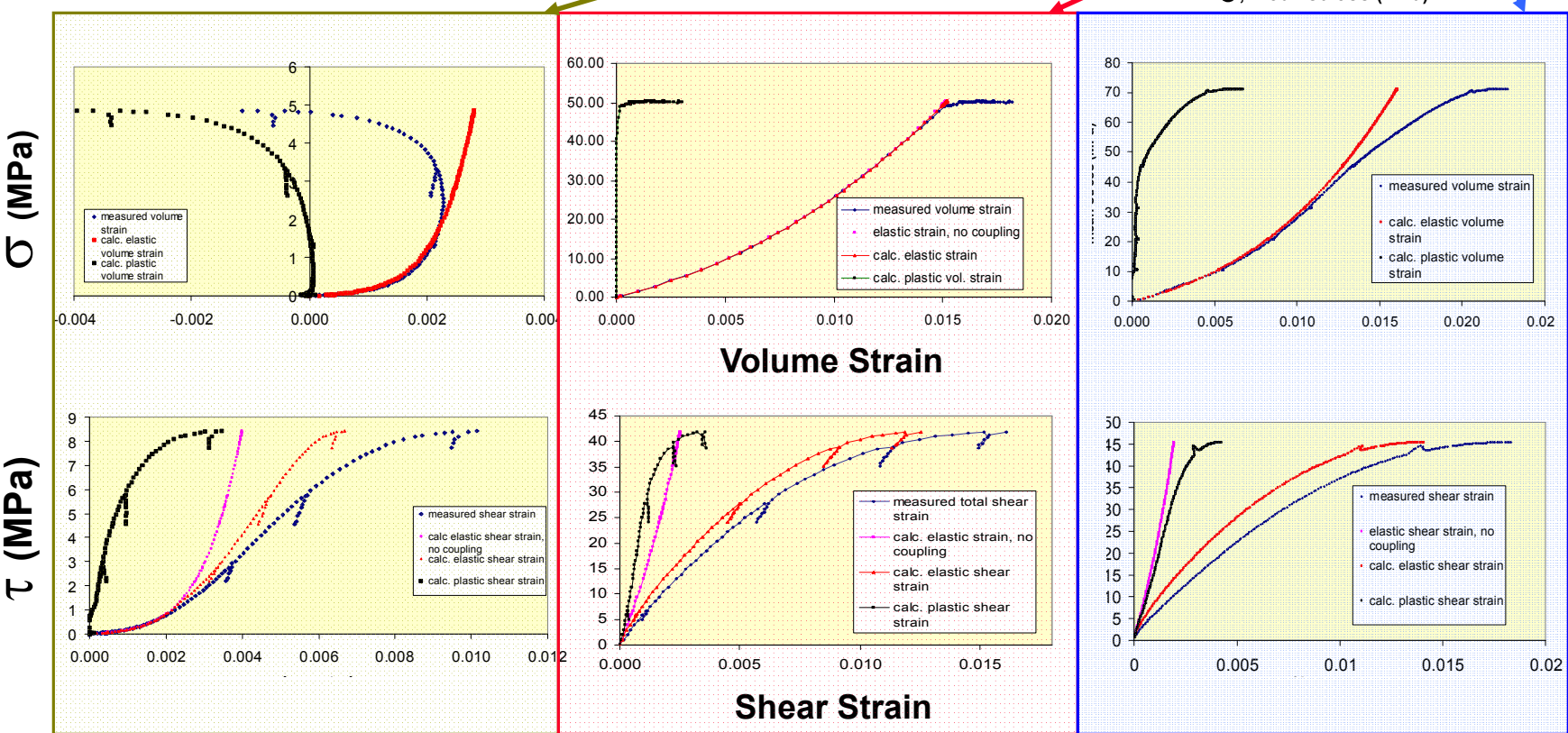


This is due to influence of microcracks (formation of which is observable by acoustic emissions, AE) on elastic bulk modulus

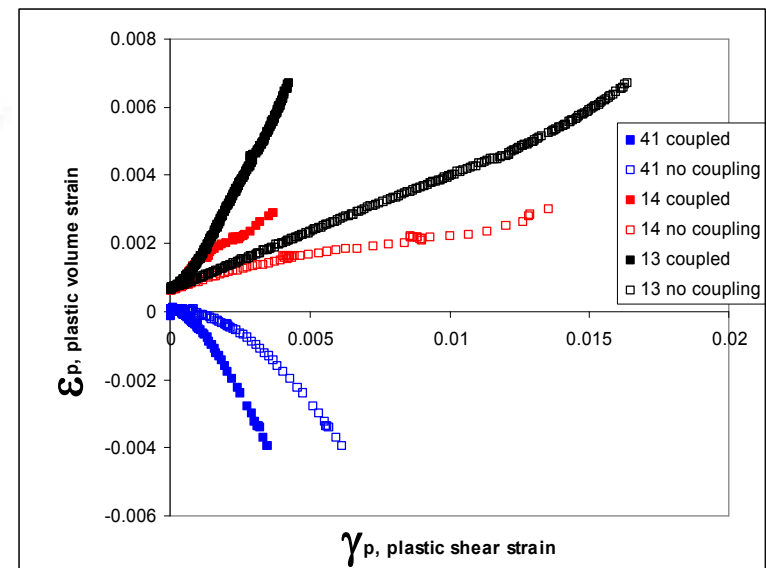
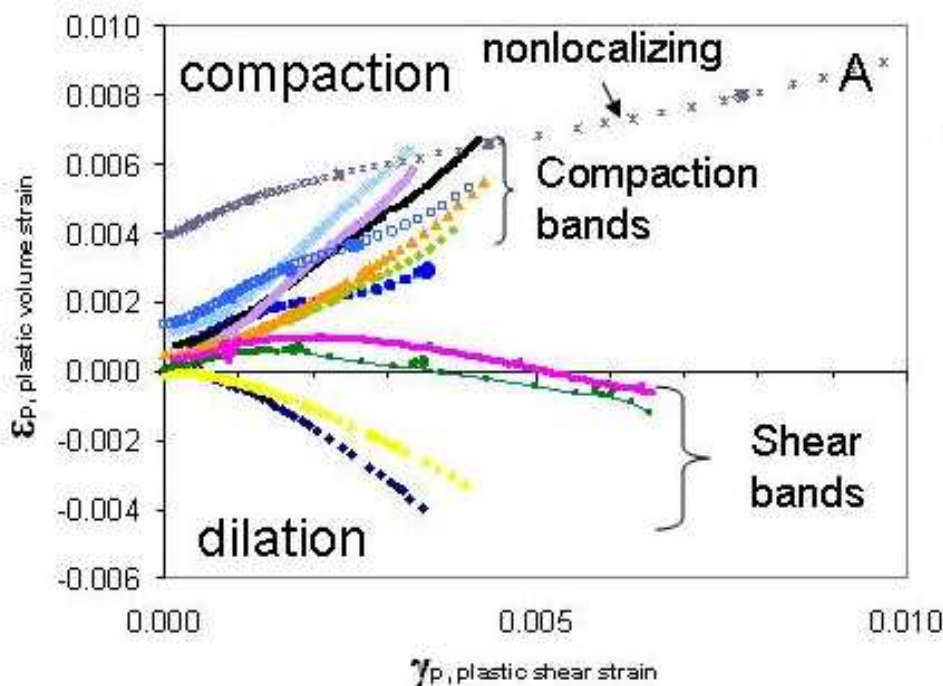
Nearly a third of total volume strain is attributable to elastic-plastic coupling in this experiment



More Examples

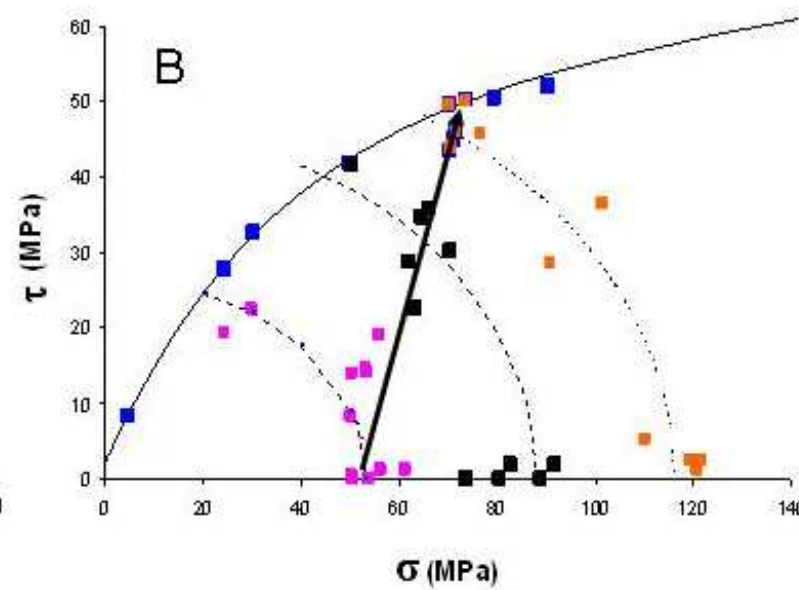
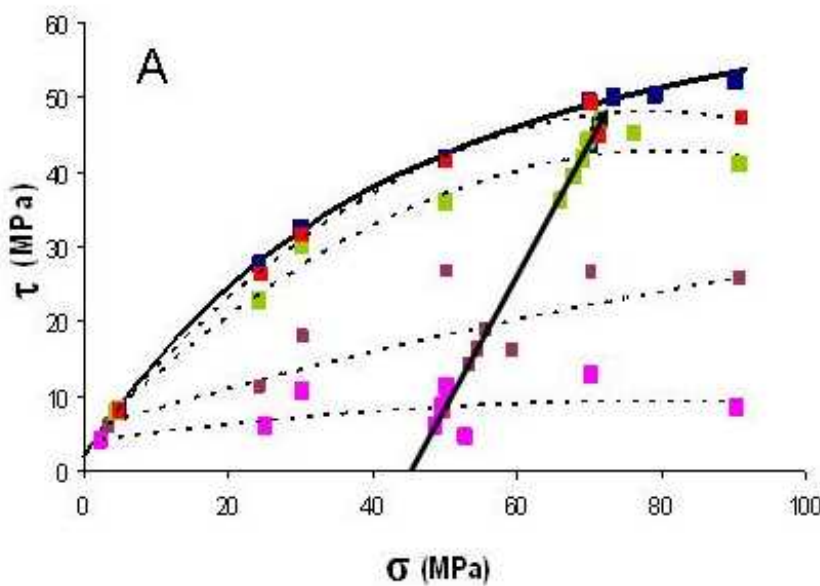


β calculation



β 's are slopes of strain paths. Ignoring coupling overestimates plastic shear strain and underestimates β

μ calculation



μ is slope of yield surface, here taken to be
contour or constant plastic shear strain (A) or
contour of constant plastic volume strain (B)

Localization Parameters and Band Angles for Castlegate

Elastic-Plastic Coupling

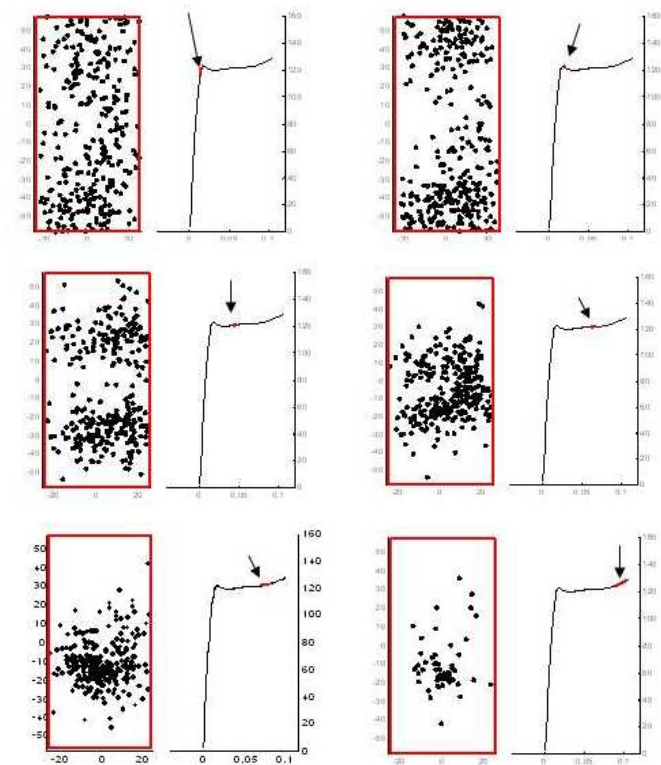
exper.	β	μ	ν	G	h_{cr}	θ
41*	1.10	0.91	0.24	4815	-4823	69.0
14*	-0.74	0.42	0.18	4597	389	34.4
13b#	-2.17	-0.36	0.29	4424	2360	0.0

No coupling

41*	1.15	1.02	0.12	8058	-7626	66.6
14*	-0.26	0.42	0.14	8918	-1397	40.1
13b*	-0.73	0.21	0.15	9263	353	31.3
13b#	-0.73	-0.36	0.15	9263	-396	22.2

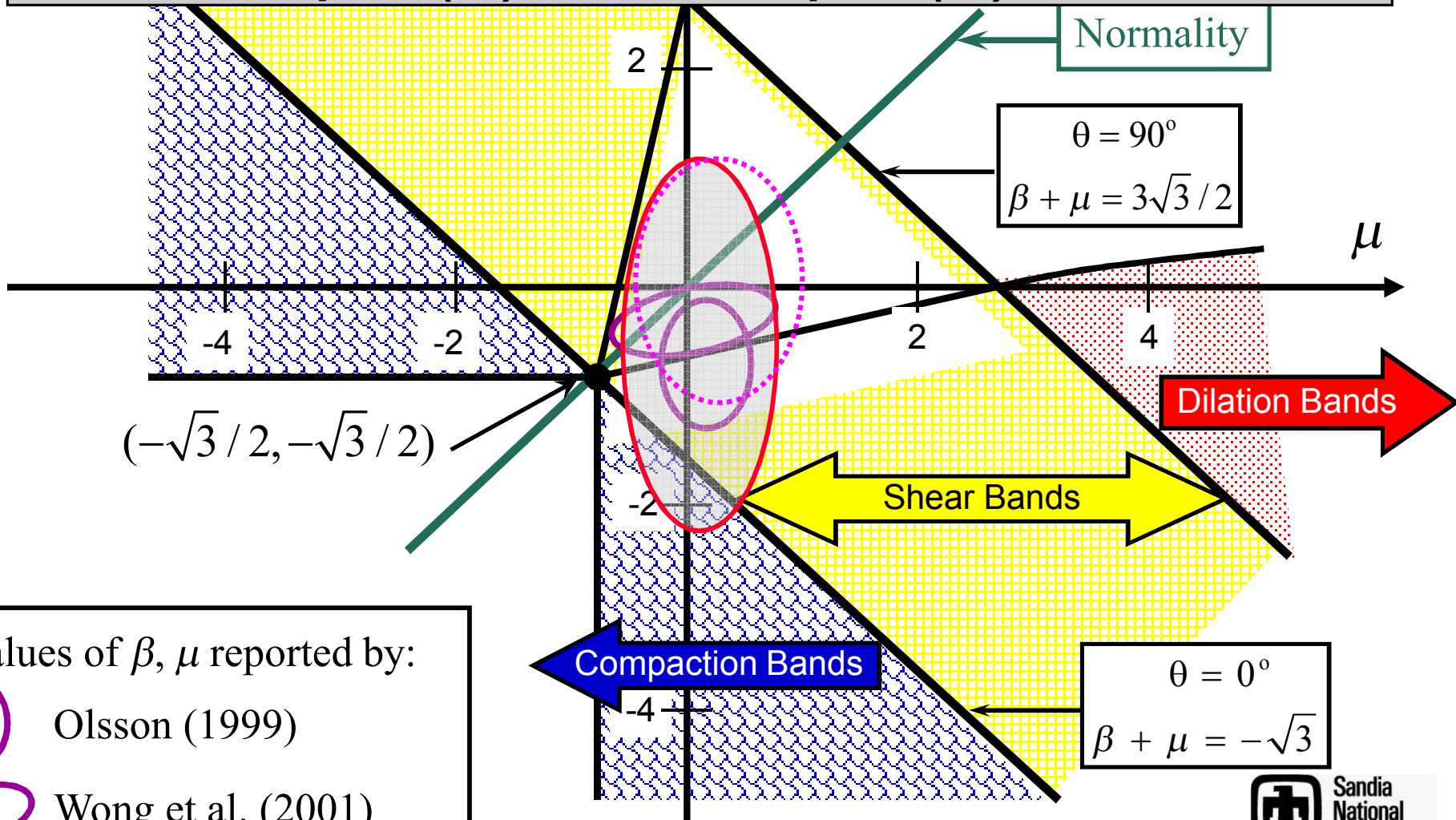
* μ and h_{cr} calculated assuming shear yield surface
μ and h_{cr} calculated assuming cap yield surface

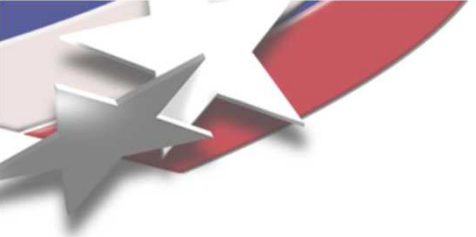
θ is in degrees, G and h_{cr} in MPa



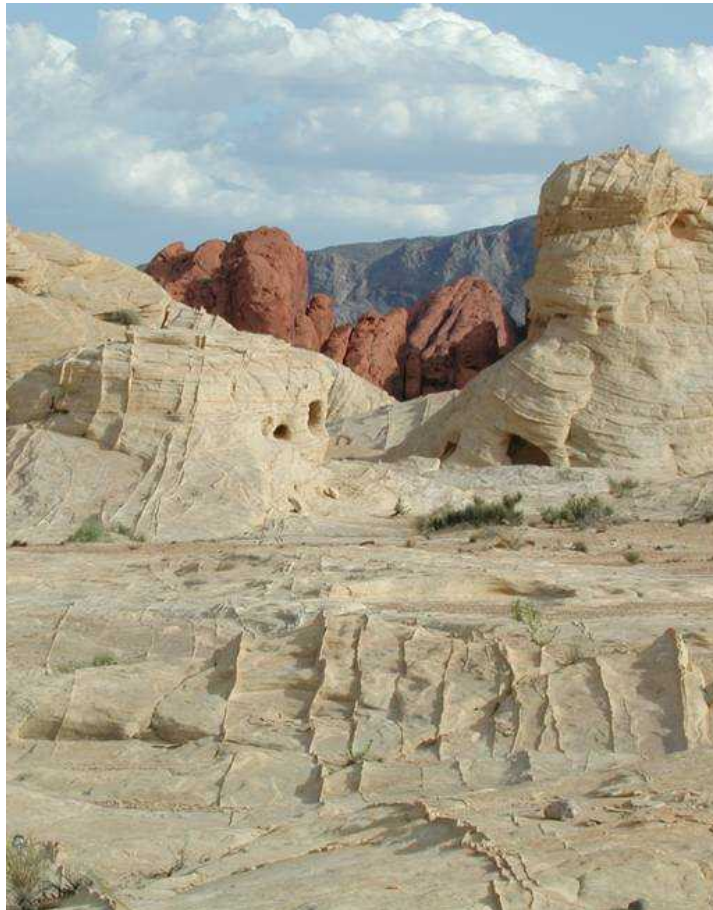
In situ band orientation determination by AE locations (exper. 13)

Range of Observed β and μ for Castlegate Experiments: Coupled (---) And Uncoupled (—) Cases





Conclusions



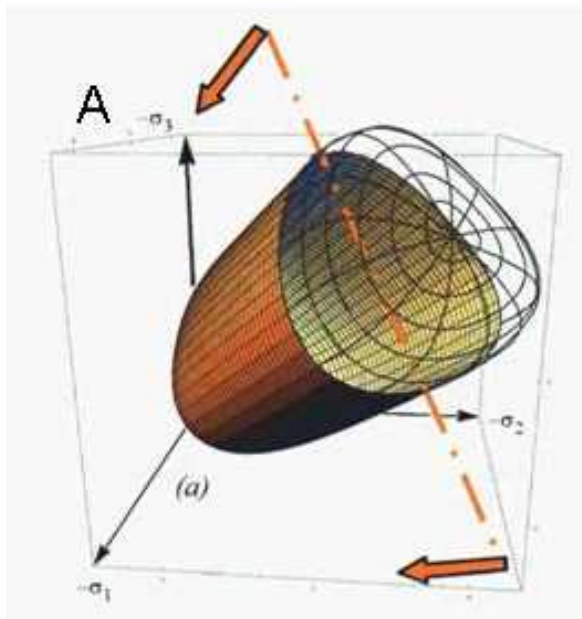
Sternlof et al., 2004

- Observed degradation of elastic moduli with plastic deformation
- Elastic-plastic coupling influences localization predictions
- First time localization theory has successfully predicted occurrence of compaction localization in experiments, using experimentally determined constitutive parameters.

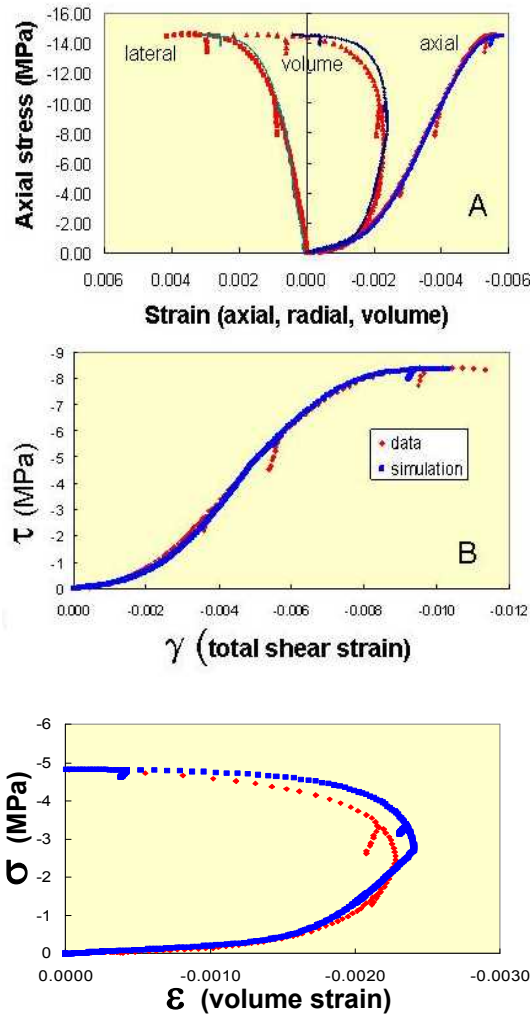


Sandia Geomodel

- Elastic parameters (tangent moduli)
- Hydrostatic Pore Collapse
- Limiting Shear Surface (incl. kinematic hardening)
- Cap Curvature
- Non-associative plastic flow



Geomodel Simulations of Castlegate Experiments



Yield and Failure Surfaces

